

Rotational Instabilities and Axial Currents
in the Theta Pinch ISAR I

M. Kaufmann, E. Fünfer, J. Junker

J. Neuhauser, U. Seidel

IPP 1/123

Oktober 1971

MAX-PLANCK-INSTITUT FÜR PLASMAPHYSIK

GARCHING BEI MÜNCHEN

MAX-PLANCK-INSTITUT FÜR PLASMAPHYSIK
GARCHING BEI MÜNCHEN

Rotational Instabilities and Axial Currents
in the Theta Pinch ISAR I

M. Kaufmann, E. Fünfer, J. Junker

J. Neuhauser, U. Seidel

IPP 1/123

Oktober 1971

*Die nachstehende Arbeit wurde im Rahmen des Vertrages zwischen dem
Max-Planck-Institut für Plasmaphysik und der Europäischen Atomgemeinschaft über die
Zusammenarbeit auf dem Gebiete der Plasmaphysik durchgeführt.*

Abstract

Rotation of the plasma column and rotational instabilities were studied in the ISAR I linear theta pinch using two coils with a length of 1.5 and 5.4 m respectively ($T_e \leq 450$ eV, $E_i \leq 4.5$ keV, n_e some 10^{16} cm $^{-3}$).

A possible mechanism which can cause plasma rotation is short-circuiting of the radial electric Hall field over the ends of the linear pinch. The axial short-circuit current predicted by this model could, in fact, be measured by measuring its magnetic field. The sign of this current and the total charge of the current pulse were in agreement with this model. The duration of the current pulse was about equal to the transit time of a torsional Alfvén wave over half the coil.

These results justify the assumption that the plasma rotation in open-ended theta pinches is essentially caused by end effects and should therefore be of minor importance for toroidal pinches.

1. Introduction

In theta pinches, rotation of the plasma column has often been observed [1 - 7]. In many cases rotational instabilities in the form of elliptical deformation of the cross section have appeared. Sometimes these instabilities have even led to splitting of the column into two or more arms rotating around one another. The ($m = 1$) instabilities also observed in theta pinches were connected with rotation and are a possible unstable rotational mode [6, 26].

The rotation of the contour of the plasma column does not strongly justify the conclusion that the bulk of the plasma is rotating. But measurements of Doppler shifted impurity lines directly showed a rotating plasma in some cases [5]. We shall revert to this problem later.

A lot of theoretical work has been done to explain rotation and rotational instabilities in the theta pinch [1, 2a, 4, 8-15]. A fairly complete discussion of different possible reasons for rotation has been given by Haines [10]. One of the different mechanisms proposed is short-circuiting of the radial electric Hall field over the ends of the pinch [2a]. It is attempted here to decide whether this mechanism is working or not.

The principle of our experiment was to measure the axial short-circuit current at the end of a theta pinch by measuring its magnetic field. Special care was taken to confirm the correlation between this current and the outflowing plasma. Our experiment was conducted on the 5.4 m long coil of the Isar I bank. A comparable measurement on a rather short coil (20 cm) was done independently by Thomas [16].

The experimental results will be discussed and compared with rough estimates based on the short-circuit model. Before the method and results of the axial current measurements are presented, a brief summary of observations of rotational instabilities in the Isar I bank is given.

2. Bank and plasma parameters

Here the main data of the apparatus and the plasma parameters of the cases investigated are given. Further details can be found elsewhere [7,17,18]. Experiments were made on the Isar I bank with two coils 1.5 m and 5.4 m in length [19,20]. In all cases the theta pinch discharge was carried out without any bias field. The plasma was preionized by two z-pinch discharges [21-23]. The main bank parameters are given in the following table:

Arrangement	IA	IB	IIA	IIC	
capacitance	1.1	3.3	1.1	3.3	mF
total inductance	21.5	15	16.5	10.3	nH
maximum voltage	30	40	30	40	kV
maximum magnetic field	59	146	16	45	kG
coil length		1.5		5.4	m
coil diameter		10.6		19.6	cm
tube diameter	8.3 ... 9		17		cm

Table 1

The plasma parameters were measured by Mach-Zehnder interferometry, laser light scattering, neutron detection, diamagnetic loops, and measurement of the continuum radiation [7,17]. Plasma parameters of four main cases investigated are given in the following table:

Arrangement	IA	IB	IIA	IIB
Voltage	30	40	30	30 kV
Bank energy	0.5	2.6	0.5	1.5 MJ
Coil length	1.5		5.4	m
Filling pressure	10		10	micron D ₂
E _{i,max}	0.8	4.5	0.2	0.85 keV
T _{e,max}	0.35	0.45	0.2	0.35 keV
n _{e,max}	2x10 ¹⁶	2x10 ¹⁶	1.7x10 ¹⁶	2x10 ¹⁶ cm ⁻³
r _{plasma} (t = 7 μs, n = 0.5 n _{max})	0.5	0.5	1.5	0.9 cm
t (n = n _{max})	5	4	7	10 μs

Table 2

3. Observations of rotational instabilities

Observations of rotational instabilities with the 1.5 m and the 5.4 m long coil are presented here. The instabilities were observed side-on with a Mach-Zehnder interferometer [17,24]. The different observations gave information about the unstable mode ($m = 1, 2 \dots$), the rotational frequency, the direction, and the onset along the axis (z -direction).

In discharges with the short coil elliptical ($m = 2$) deformation of the plasma was observed by means of stereoscopic smear pictures. While the amplitude of this deformation was limited to the order of the plasma radius, the frequency of the rotation increased with time. A typical smear picture is shown in Fig. 1. Only occasionally a rotational ($m = 1$) deformation was observed (Fig. 2). End-on interferograms showed the elliptical deformation of the plasma cross section, too. To get the rotational frequency, a narrow rectangular

aperture (slit) perpendicular to the fringes of the interferogram was smeared by a rotating mirror. The rotating, elliptically deformed plasma column caused oscillation of the fringes in this smear interferogram (Fig. 3). It can be seen that the outer and inner regions of the column have the same rotational frequency.

The frequencies of side-on and end-on smear pictures agreed within the statistical error. Results are given in Figs. 4 and 5. In Fig. 4 rotational frequencies of ($m = 2$) modes of discharges with two different energies are compared as functions of time. Higher ion temperature of the plasma was connected with higher rotational frequency, in both cases increasing with time. For comparison the rotational frequency corresponding to a velocity equal to the ion thermal velocity at $r = 1$ cm is marked, too. It can be seen that the rotational velocity is below, but of the order of the ion thermal velocity.

Figure 5 shows results obtained under conditions where both ($m = 2$) and ($m = 1$) instabilities were observed. At a later time in the ($m = 1$) case a lower frequency appeared. On the other hand a larger radius of the rotating mass may give about the same angular momentum.

While the rotational instabilities in the short coil experiments were limited to amplitudes of the order of the plasma radius, in the long coil there was, in general, a sharp onset and growth of the radius. There existed a general tendency towards modes with higher m -numbers ($m \geq 2$) at low ion energy and vice versa.

Typical smear pictures are given in Fig. 6a,b. At higher pressure (15μ), and hence lower ion temperature, a well developed ($m = 2$) instability and, in the other case, a ($m = 1$) instability appeared. The onset time of the instabilities in the long coil was investigated as a function of z . No clear dependence on the position along the axis could be found. The instabilities may appear somewhat earlier in the middle than at the ends. Also the rotational frequency showed no dependence on z . Only the amplitude seemed to be smaller at the ends.

The direction of the rotation could be determined by stereoscopic smear pictures in all cases where a ($m = 1$) mode developed or the

arms of a ($m = 2$) mode were of different brightness. In all these cases the observed direction agreed with the direction of a diamagnetic ion current. Finally, we briefly discuss the question whether the rotational velocity observed in the contour of the plasma (phase velocity) is identical with or near the velocity of the bulk. If the difference of the velocities is large, much energy would be needed for permanent deformation of the plasma and the source of this energy could only be a strongly growing mode. This means, on the other hand, in all cases where the amplitude of the deformation is nearly constant in time the mass velocity must be very close to the phase velocity. This argument is especially valid in cases with ion-ion collision times of several μ s or less.

Summarizing, it can be stated that under nearly all conditions more or less reproducible rotational instabilities could be observed. The velocity was of the order of the ion thermal velocity and the direction identical with that of a diamagnetic ion current.

4. Z-current measurement

a) Principle of the measurement

A compressed theta pinch plasma with zero angular momentum means that the azimuthal current is essentially an electron current. The force proportional to $\vec{j} \times \vec{B}$ in the radial direction therefore acts only on the electrons. The ions will be coupled and held together by an electric field. In the MHD equations this field appears as the Hall field.

If this Hall field perpendicular to the magnetic field is constant along the field lines, equilibrium is possible. On the other hand, in a theta pinch of finite length the condition of constant Hall field will, in general, not be satisfied. Especially where the magnetic field lines go through the vacuum vessel, the cold plasma may be rather dense. At the surface the Hall field is therefore very low, and the electric field is nearly short circuited. This must lead to a current flowing along the field lines and finally to zero electric field all over the theta pinch. This again means that each sort of

particles p must carry a current \vec{j}_p such that $(\vec{j}_p \times \vec{B})$ balances the pressure gradient of these particles. A diamagnetic ion current is identical with rotation of the plasma column.

Without going into all the details, one finds that the assumed mechanism is accompanied by a current along the field essentially in the z -direction. The purpose of the experimental work reported here was to determine whether this mechanism acts. This was done by measuring the magnetic field of this current. The schematic arrangement for this measurement is shown in Fig. 7. Details of the experiments, conducted only on the long coil, are given in the following. The experimental results then reported are followed by a discussion of the mechanism.

b) Details of the measurement

The I_z current was measured by means of its magnetic field B_φ . An induction loop inside a glass tube (outer diameter 8 mm) was therefore introduced into the discharge vessel from one end (see Fig. 7).

The magnetic loop could be rotated in two different ways (see Fig. 8). Rotation around the axis of the pinch (φ -direction), together with glass screening enabled us, in principle, to measure $B_\varphi(\varphi)$ along a circle of radius 7 cm. The averaged value $B_\varphi(\varphi)$ is exactly proportional to the current flowing through this circle. In practice, B_φ was measured at four positions with $\Delta\varphi = \pi/2$ and these values were averaged. So any asymmetry of the current I_z has been adequately taken into account.

Furthermore, it was possible to rotate the magnetic loop inside the screening (direction γ). This was necessary to guarantee in each φ -position that no disturbing part of the relatively large B_z , B_r components of the main field were picked up. The method how to get B_φ by measuring the magnetic field signal with and without plasma at different angles γ is illustrated in Fig. 8. In a third displacement it was possible to shift the loop together with the screening in the z -direction. This variation was used to determine the position with maximum B_φ -field. In this place the axial plasma current goes through its zero point.

Together with the magnetic measurements photographs of the out-streaming plasma were made side-on to get information about the correlation between the local distribution of the axial current and the outstreaming plasma.

c) Experimental results

Investigations were carried out on the 5.4 m coil at 0.5 MJ bank energy with 10 micron D_2 filling pressure and 1.5 MJ energy with 6 to 20 micron pressure. Figure 9 (top) shows a typical oscillogram of the B_φ (i.e. I_z) signal. For comparison I_θ is recorded below. The upper trace records a non-zero signal already before ignition of the theta pinch. This is the z-current of the preionization. By nonlinear resistances in the preionization circuit this z-current is damped out just at the ignition of the main discharge.

During the thetapinch phase a pronounced B_φ pulse could be observed about 5 to 10 μ s after ignition. The direction of the corresponding current I_z was in agreement with the assumption of short circuiting of a radial Hall field. Large B_φ values were measured about 20 to 50 cm outside the coil.

In the region with high B_φ signals the outstreaming plasma was observed to contact the tube wall. Figure 9 (bottom) shows an image converter picture of the tube outside the coil. Coil, tube, and a metal flange are drawn schematically. Inside the tube a luminous ring can be seen. The position of the magnetic probe, in the experiment 250 mm outside the coil, is indicated by a dark strip on the outer surface of the tube. The probe itself produced a dark spot on the luminous ring. The ring could also be observed without the probe. The picture in the lower part of Fig. 9 was taken with an exposure time of 1 μ s at the maximum of I_z as indicated in the oscillogram above.

A more detailed comparison between the spatial distribution of B_φ at various times and the positions of the luminous ring in the same time regime is shown in Fig. 10. The appearance of the ring coincides with the maximum of B_φ in time and space. Under the condition $E_0 = 0.5$ MJ and $p_0 = 10$ micron D_2 the time lag of 8 to 15 μ s is just the time of maximum B_φ and of the most pronounced appearance

of the luminous ring. At earlier times no comparable ring could be observed. This probably explains the fact that in short coil experiments no such phenomenon has been observed.

With the same bank energy ($E_0 = 1.5$ MJ) investigations were made with different filling pressures of $p_0 = 6, 10, \text{ and } 20$ micron D_2 . Results of these I_z current measurements are shown in Fig. 11. All measurements were made with the same z-position of the probe 25 cm outside the coil. This was the position of maximum B_ϕ at $E_0 = 1.5$ MJ. A luminous ring was again observed at the same place.

In the preionization phase the probe recorded the current of the z-pinch. Comparison with a net z-current measurement in the outer circuit of the z-pinch showed that the net current was already damped out while a current was still flowing inside the plasma.

This short-circuit current has already been observed [22]. But under all conditions the remaining current was small compared with the z-current produced by the theta pinch.

A pronounced pulse of z-current appeared 3 to 6 μs after ignition of the theta pinch, reaching the maximum after 4 to 10 μs . Both time lags increased with increasing pressure. The error of the maximum value of the current was about $\pm 20\%$. The z-current reached 25 kA in the case $p_0 = 6$ micron D_2 , $E_0 = 1.5$ MJ.

d) Discussion of the z-current measurements

The assumption of an electrical Hall field in the boundary layer of the theta pinch means that the inner part of the pinch column is negative with respect to the outer region. Consequently, short circuiting of this field should lead to a current flowing to the ends of the coil in the outer region and inward in the inner region (see Fig. 7). This was just the direction observed in the experiments.

With respect also to magnitude and duration of the current pulse a rough agreement between the hypothesis and the experiments could be obtained.

The assumption of a short circuit implies that the ion gas expands in the radial direction roughly over a distance equal to the ion gyro-radius [11]. The charge of this volume is roughly:

$$Q \approx 2 \pi r_g r_{1/2} \frac{L_p}{2} \frac{n_A}{2} e$$

r_g ion gyro-radius

$r_{1/2}$ radius with $n(r_{1/2}) = \frac{n_A}{2}$

n_A density on the axis

L_p plasma length

In the case of purely 2-dimensional compression Q is constant in time.

Considering the long coil experiment with a bank energy of 1.5 MJ and 10 micron D_2 (arrangement IIB) and taking the plasma parameters of Table 2, one gets:

$$Q \approx 0.36 \text{ As .}$$

On the other hand, the experimental value of the I_z current pulse under the same conditions was:

$$Q \approx 0.17 \text{ As .}$$

Considering the rough assumptions and the fact that measurement of Q at a fixed z -position only gives a minimum value, the agreement seems to be satisfactory.

The short circuit inside the plasma column should propagate with Alfvén speed. Therefore the Alfvén transit time over half the coil length should give a lower limit for the I_z current pulse duration. The Alfvén transit time for the above case ($E_0 = 1.5$, 10 micron D_2) at the mean plasma radius and maximum compression was:

$$t_A = 6.5 \text{ } \mu\text{s.}$$

For comparison the time between the ignition of the main discharge and the maximum of I_z was

$$t_{\text{exp}} = 8 \text{ } \mu\text{s} .$$

Especially as regards the time scale, the experiment here differs from that conducted on Scylla IA [16]. While the total coil length in the latter experiment was 20 cm and hence the transit time was less than the rise time of the magnetic field, here in the Isar I experiment both times were about equal.

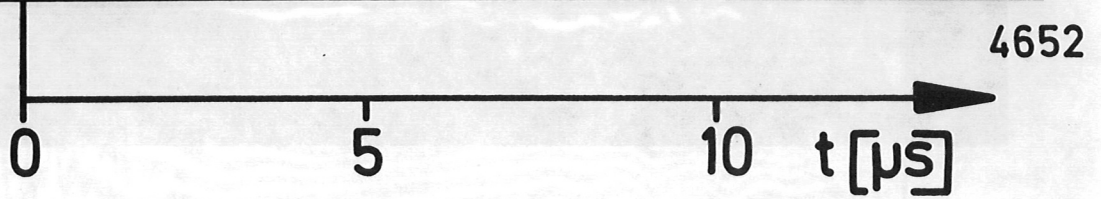
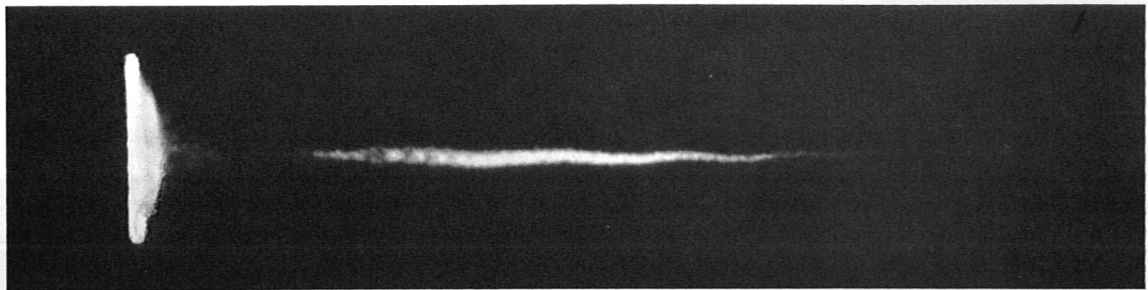
To understand the propagation mechanism of the short circuit and the associated transport of mechanical momentum in greater detail, one has to realize that the Alfvén speed varies very rapidly in the boundary layer of a theta pinch. It may be possible that in the outer region of the pinch the rotation of the ions sets in almost at once. Furthermore it may be possible that the angular momentum is transported inward by viscosity as is assumed in the rigid rotor model [25]. This would explain the fact that up to now no sharp front of a wave transporting the rotation from the ends has been observed. On the contrary, rotational instabilities indicate a constant rotation all along the length, which would be explained by the above assumption.

Summarizing, we have shown by measurement that the rotation of a straight theta pinch is accompanied by an axial electric current. This current is set up by shortcircuiting the radial electric field (Hall field) at the ends of the tube outside the coil where the plasma hits the wall. Details of the transport of the angular momentum should be investigated in the future.

References:

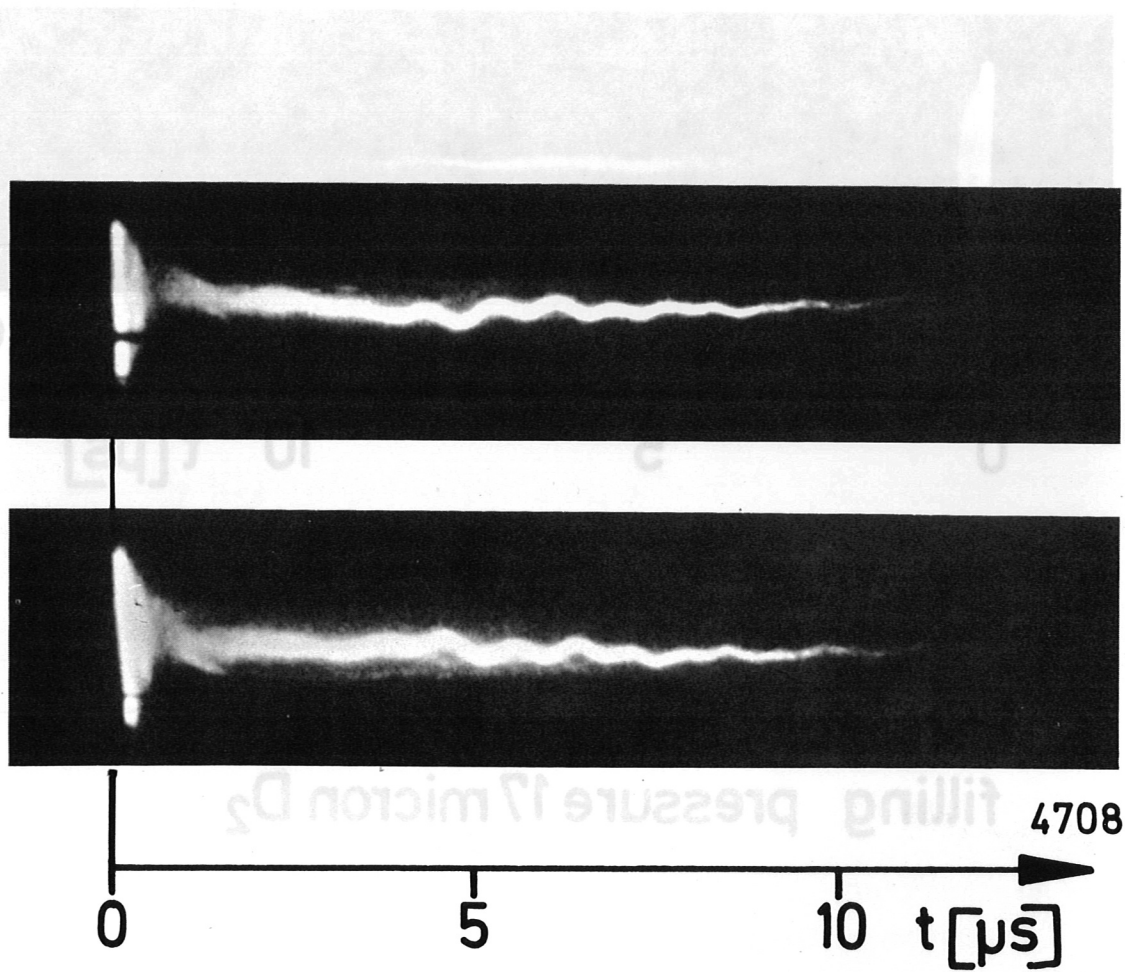
- [1] ROSTOKER, N., A.C. KOLB, Phys. Rev. 124, 965 (1961).
- [2] BODIN, H.A.B., T.S. GREEN, G.B.F. NIBLETT, N.S. PEACOCK, J.M.P. QUINN, J.A. REYNOLDS, Nucl. Fus. Suppl. 2, 521 (1962).
- [2a] ROBERTS, K.V., private communication, quoted in [2].
- [3] LITTLE, E.M., W.E. QUINN, F.L. RIBE, G.A. SAWYER, Nucl. Fus. Suppl. 2, 497 (1962).
- [4] BODIN, H.A.B., A.A. NEWTON, Phys. Fluids 6, 1338 (1963).
- [5] KEILHACKER, M., H. HEROLD, J. COOPER, D.E. ROBERTS, Plasma Phys. Contr. Nucl. Fus. Res., Culham, 1965, CN-21/54.
- [6] BODIN, H.A.B., A.A. NEWTON, T.S. GREEN, G.B.F. NIBLETT, J.A. REYNOLDS, Plasma Phys. Contr. Nucl. Fus. Res., Culham, 1965, CN-21/43.
- [7] NEUHAUSER, J., IPP Report 1/109 (1970) and Z. Phys. 245, 361 (1971).
- [8] TAYLOR, J.B. Plasma Phys. 4, 401 (1962).
- [9] ROSENBLUTH, M.N., N.A. KRALL, N. ROSTOKER, Nucl. Fus., Suppl. I, 143 (1962).
- [10] HAINES, M.G., Adv. Phys. 14, 167 (1965).
- [11] MORSE, R.L., Phys. Fluids 10, 1560 (1967).
- [12] DÜCHS, D. Phys. Fluids 11, 2010 (1968).
- [13] BOWERS, E., M.G. HAINES, Phys. Fluids 11, 2695 (1968).
- [14] BENFORD, G., Plasma Phys. 11, 787 (1969).
- [15] PALSEDGE, J.A. Phys. Fluids 12, 336 (1969).
- [16] THOMAS, K.S., Phys. Rev. Lett. 23, 746 (1969).
- [17] KAUFMANN, M., J. NEUHAUSER, H. RÖHR, IPP-Report 1/105 (1970) and Z. Phys. 244, 99 (1971).
- [18] KAUFMANN, M., E. FÜNFER, J. JUNKER, J. NEUHAUSER, IPP-Report 1/111 (1970).
- [19] KNOBLOCH, A. IPP-Report 4/12 (1964).
- [20] BREIT, E., and A. KNOBLOCH, IPP-Report 4/65 (1968).
- [21] HERTZ, W., A. KOLLER, A. MICHEL, Z. Naturf. 19a, 1089 (1964).

- [22] EBERHAGEN, A., W. KÖPPENDÖRFER, M. MÜNICH, Proc. APS-Top. Conf. Puls. High-Dens. Plasma, Los Alamos, 1967, LA-3770, H2.
- [23] KÖPPENDÖRFER, W., IPP-Report 1/79 (1968).
- [24] ANDELFINGER, C., et al., IPP-Report 1/67 (1967).
- [25] MORSE, R.L., J.P. FREIDBERG, Los Alamos Rep. LA-DC-10598, (1969).
- [26] BOWERS, E., and M.G. HAINES, Phys. Fluids 14, 165 (1970).



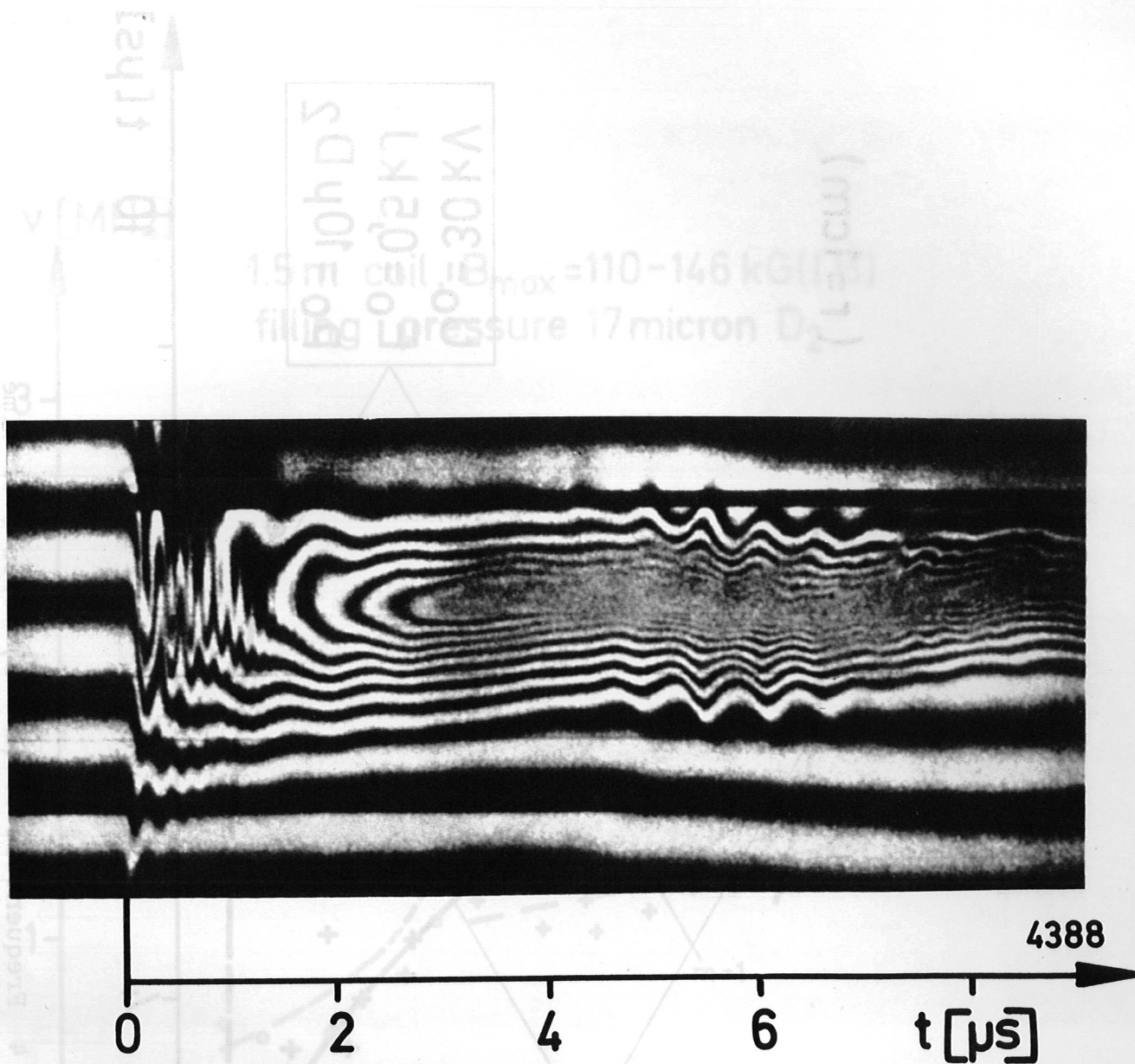
1.5m coil, $B_{\max} = 146 \text{ kG (IB)}$
filling pressure 17 micron D_2

Fig. 1 Smear picture, ($m = 2$) deformations are observable.



1.5m coil , $B_{\max} = 128 \text{ kG (IB)}$
 filling pressure 17micron D_2

Fig. 2 Stereoscopic smear picture, ($m = 1$) deformations are observable.



1.5m coil, $B_{\max} = 59\text{kG}$ (IA)
 filling pressure 10micron D_2

Fig. 3 Smear interferogram end-on.

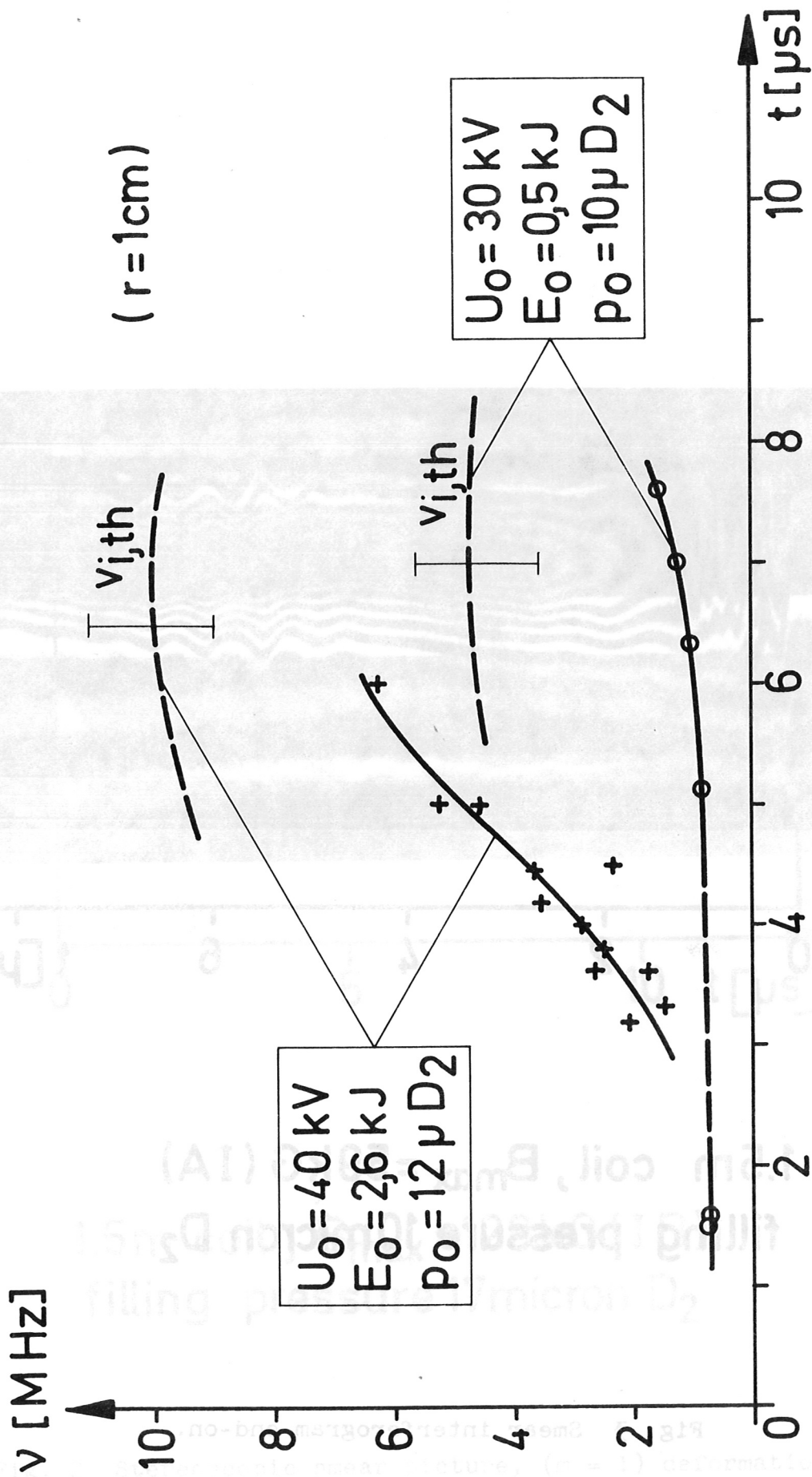


Fig. 4 Frequencies of ($m = 2$) modes over time with two different ion temperatures.

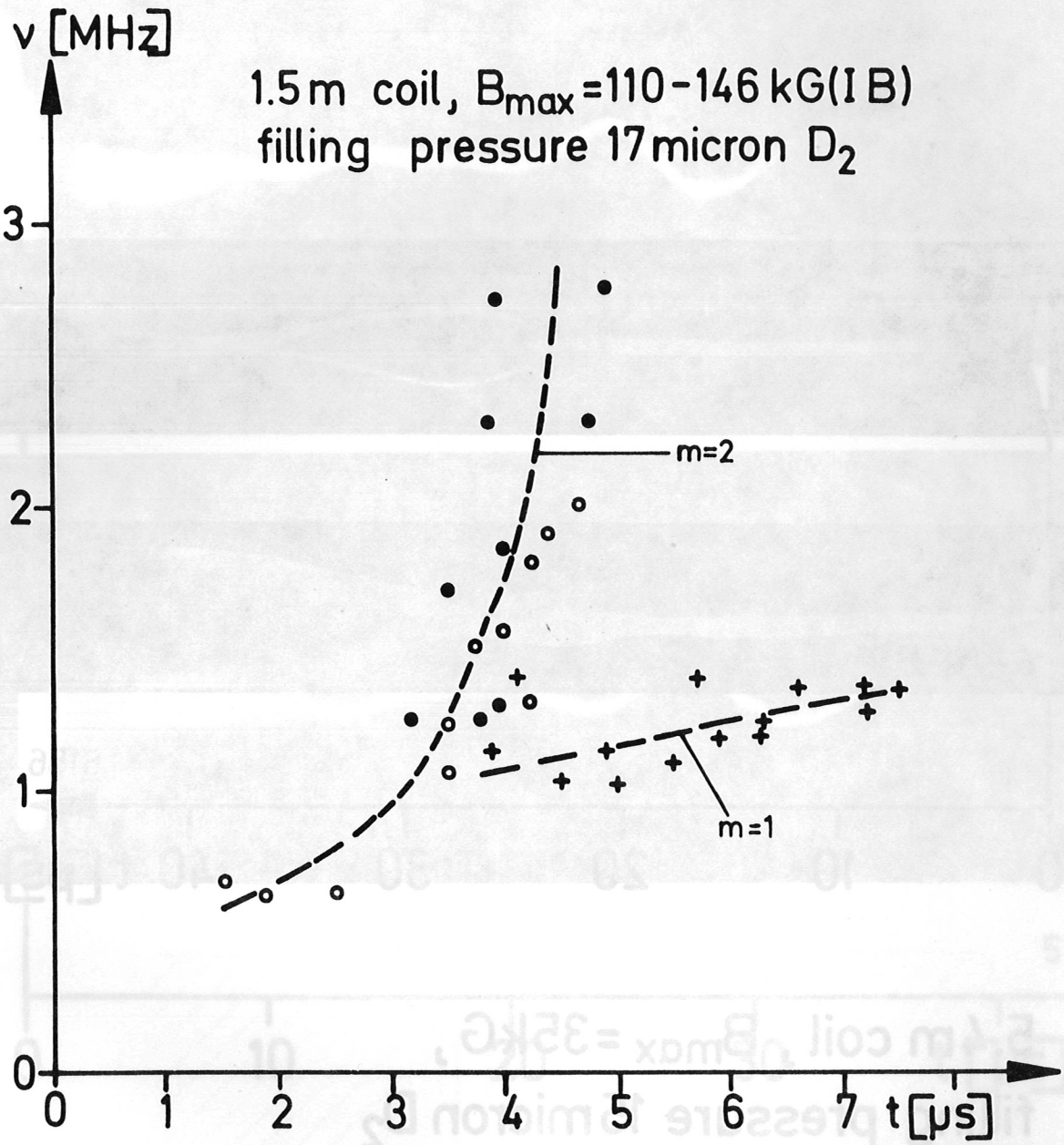
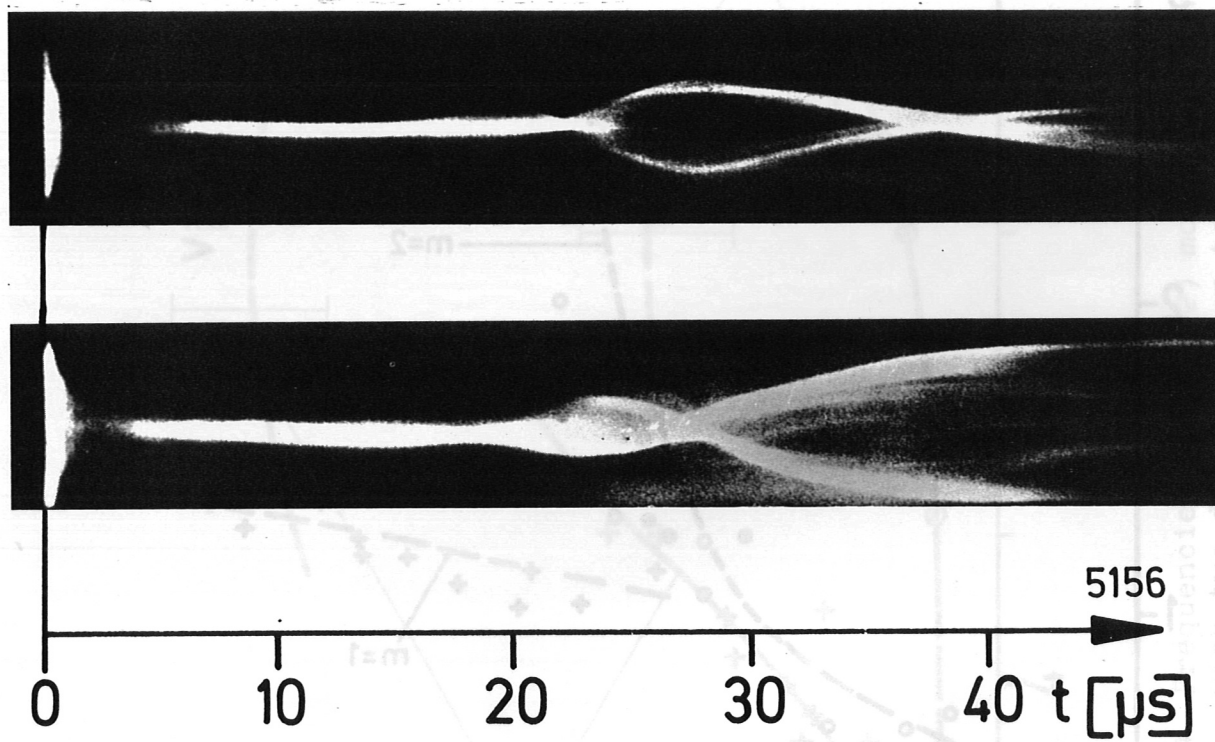


Fig. 5 Frequencies of ($m = 1$) and ($m = 2$) modes.

5.4 m coil, $B_{\max} = 35$ kG (II B)
 filling pressure 6 micron D_2

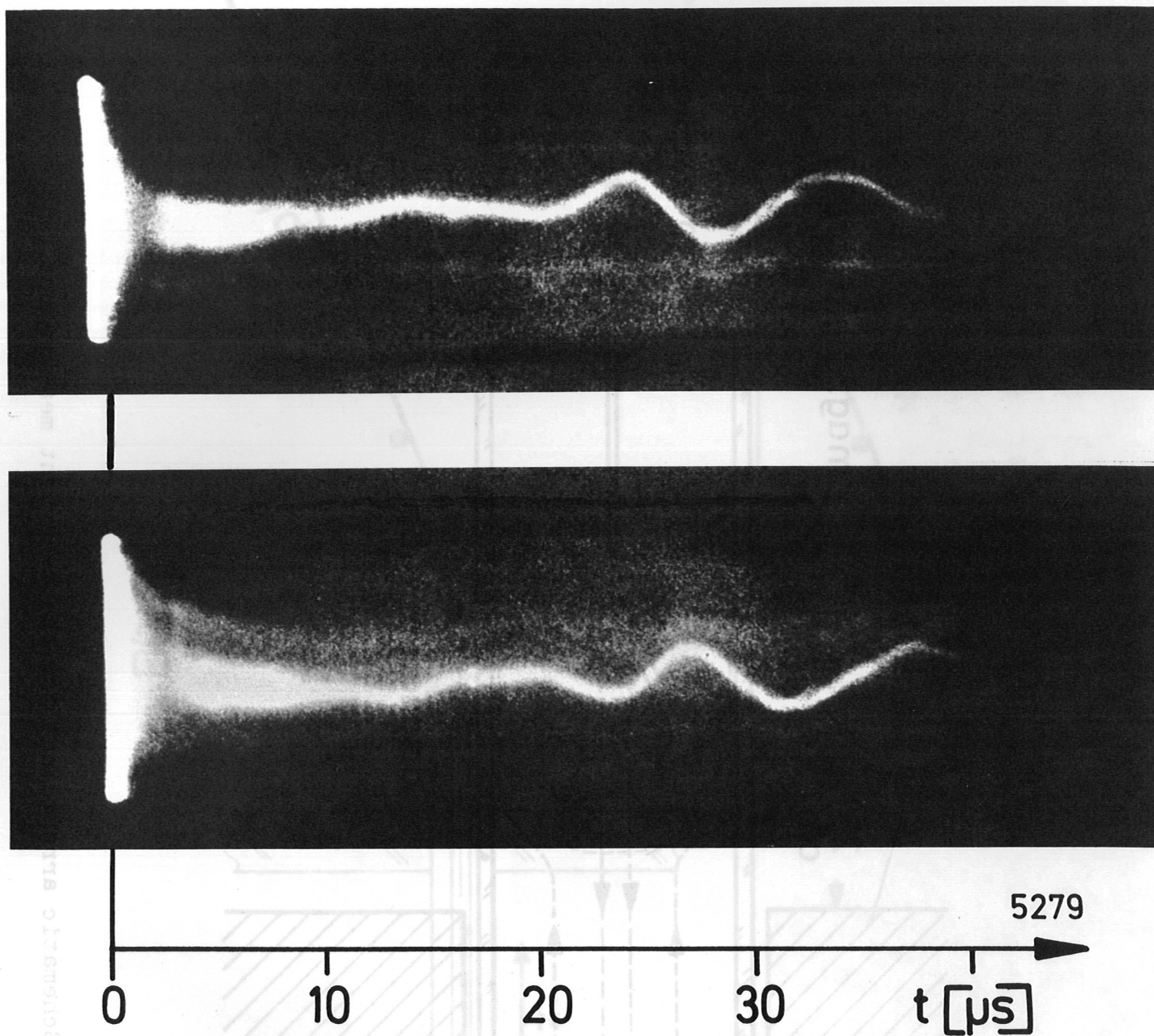
Fig. 6 Typical stereoscopic pictures of the long coil experiment.

Fig. 6b Typical stereoscopic pictures of the long coil experiment.



5.4m coil , $B_{\max} = 35\text{kG}$,
 filling pressure 15micron D_2

Fig. 6a Typical stereoscopic pictures of the long coil experiment.



5.4 m coil, $B_{\text{max}} = 35 \text{ kG}$ (II B)
filling pressure 6 micron D_2

Fig. 6b Typical stereoscopic pictures of the long coil experiment.

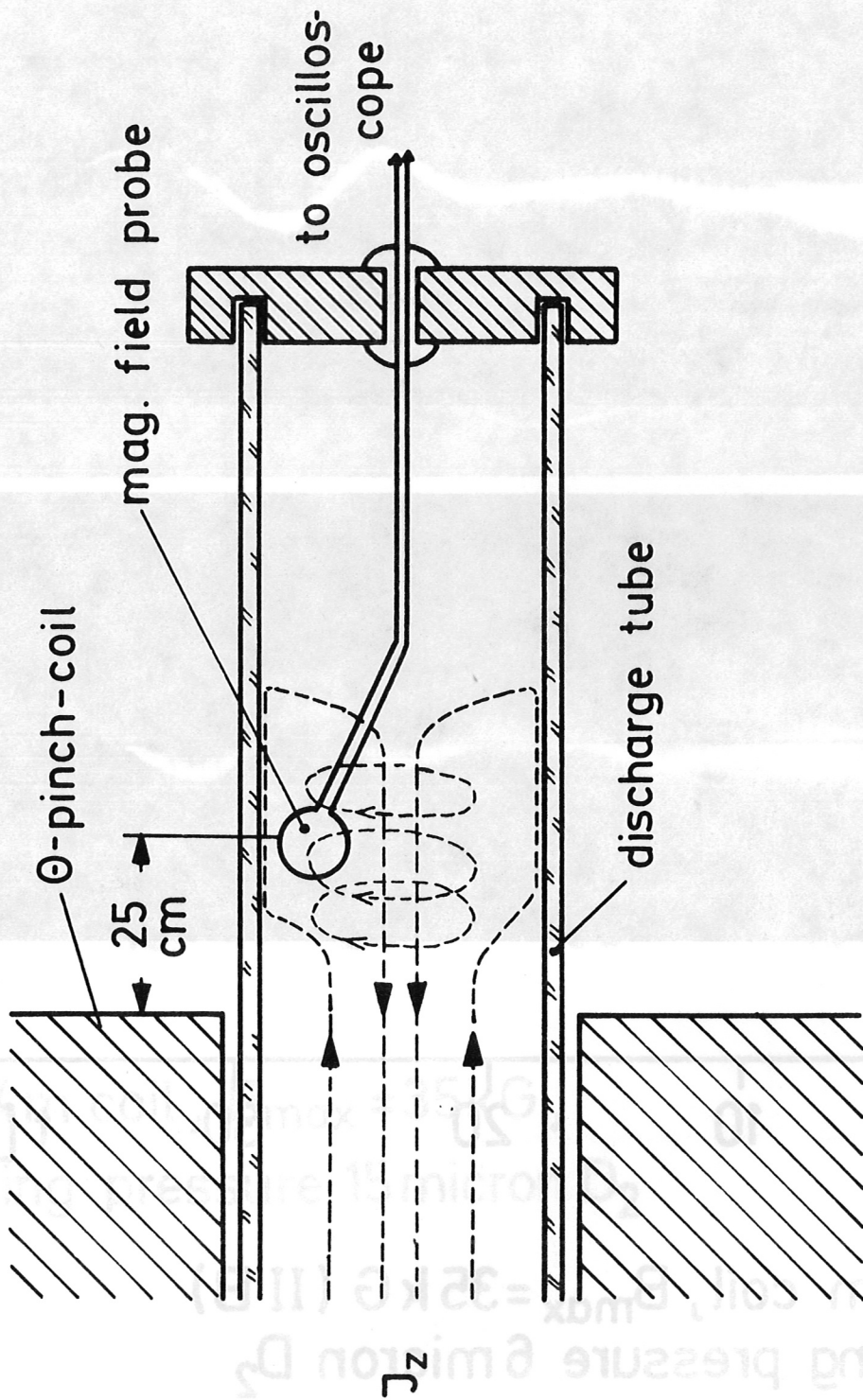


Fig. 7 Schematic arrangement for the z-current measurement.

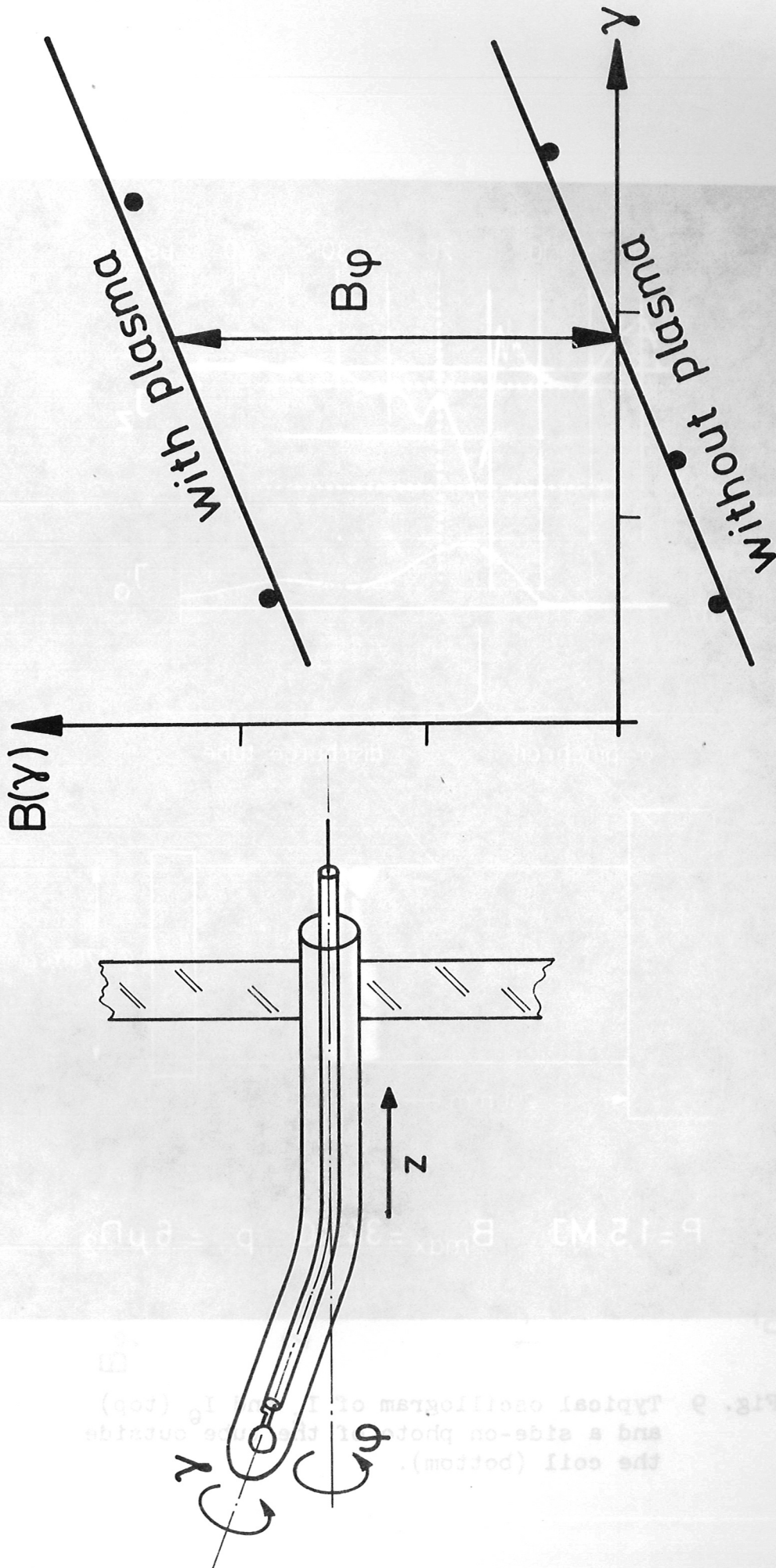


Fig. 8 Possibilities of turning the magnetic field probe.

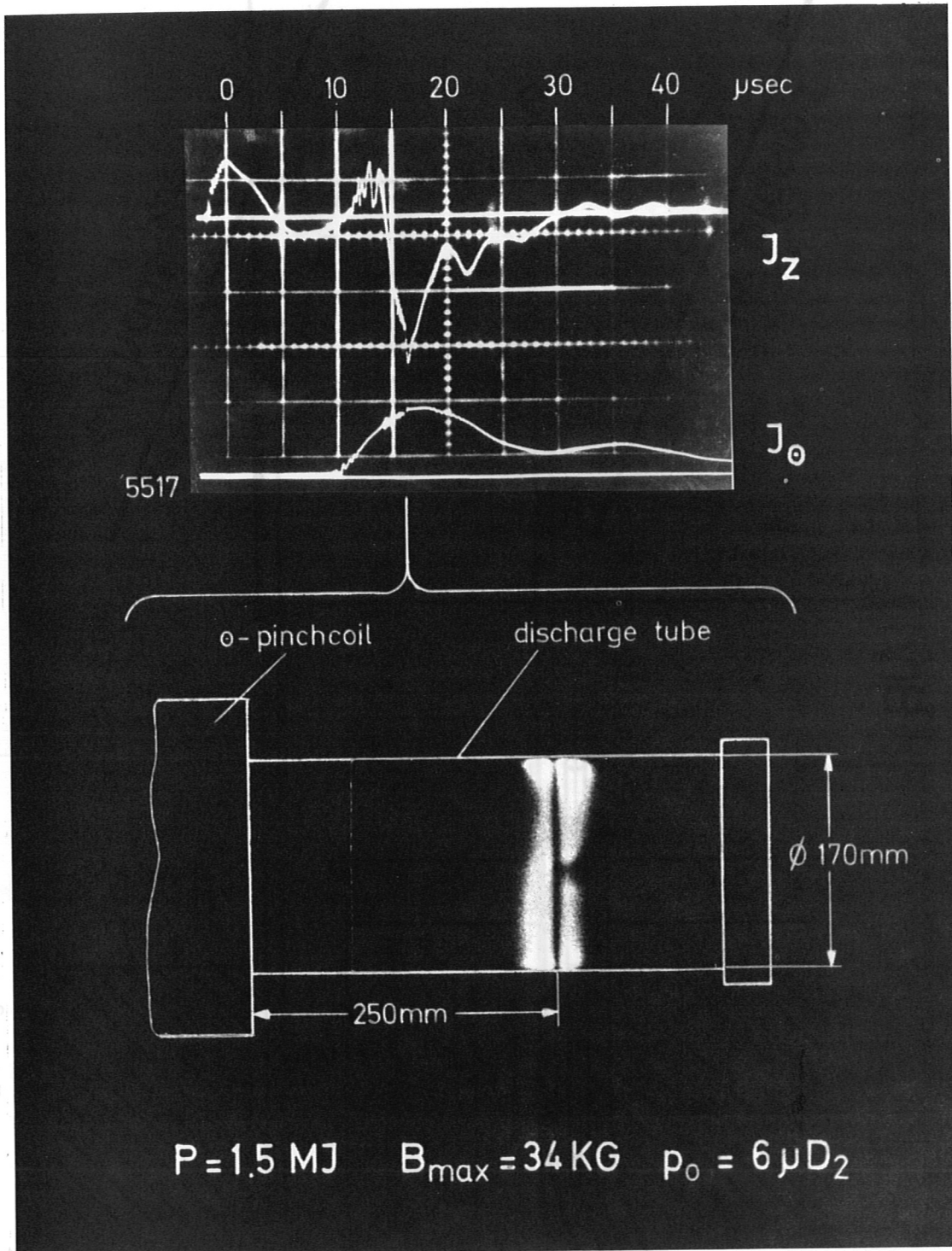


Fig. 9 Typical oscillogram of I_z and I_θ (top) and a side-on photo of the tube outside the coil (bottom).

$E_0 = 0,5 \text{ MJ}$ $U_0 = 30 \text{ kV}$ (2/6)

$P_0 = 10 \mu\text{D}2$

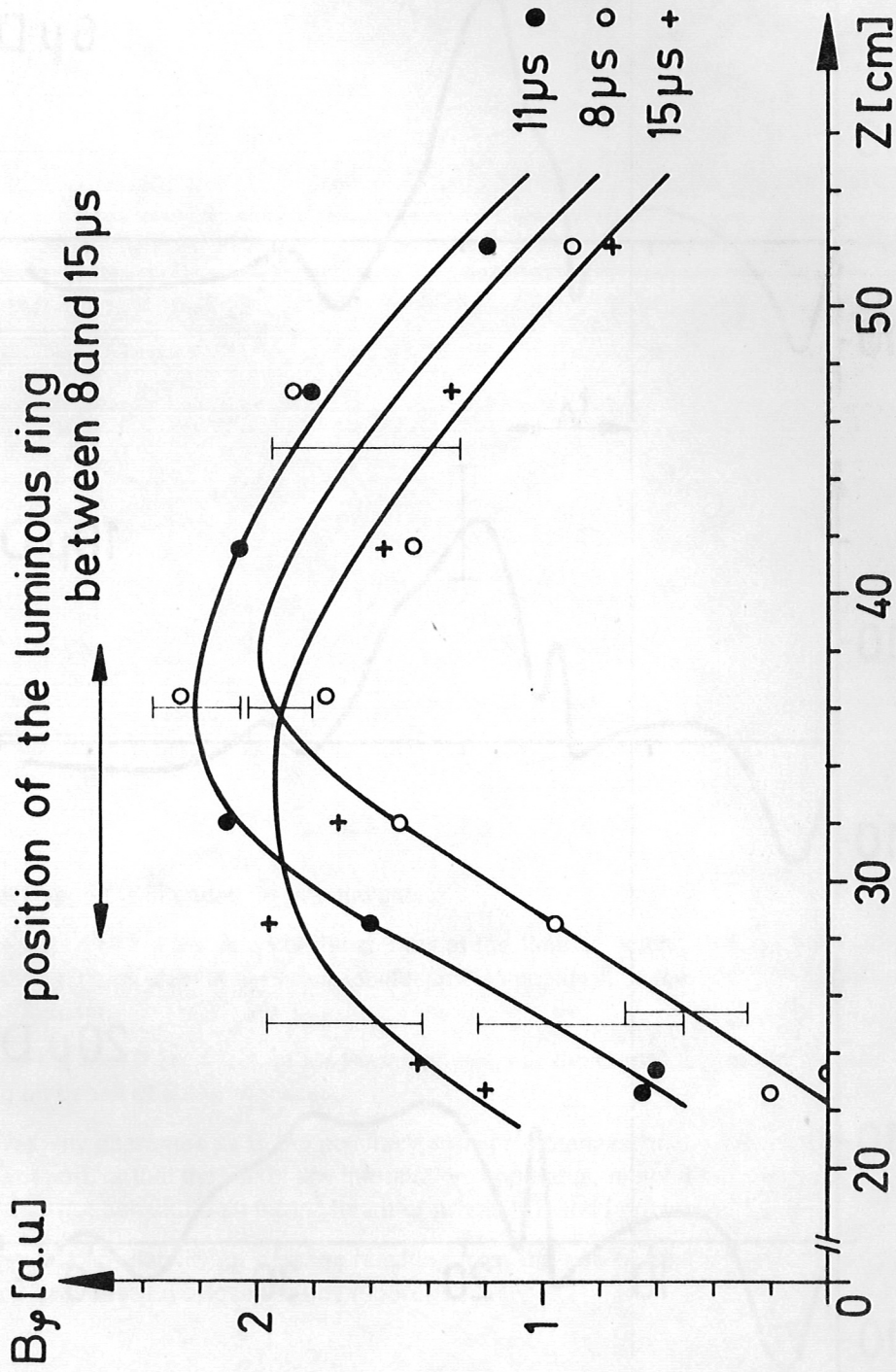


Fig. 10 The magnetic field component B_φ as a function of the z-position and time.

$E_0 = 1.5 \text{ MJ}$ 5.4 m coil (IIB)

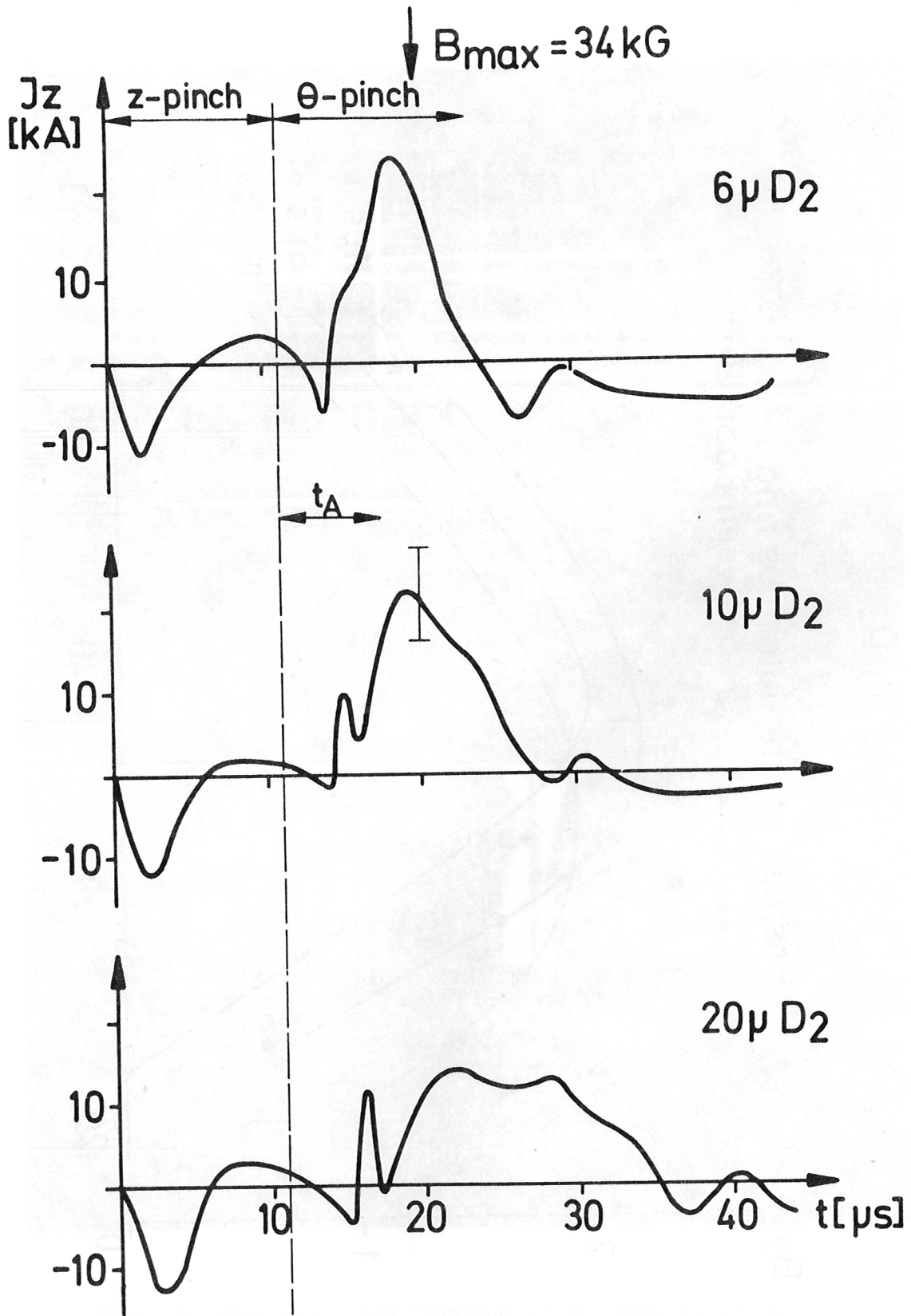


Fig. 11 The current I_z as a function of time for different filling pressures.